



Investigation of Li/Ca variations in aragonitic shells of the ocean quahog *Arctica islandica*, northeast Iceland

Julien Thébault

Earth System Science Research Centre Geocycles and INCREMENTS, Department of Applied and Analytical Paleontology, Institute of Geosciences, University of Mainz, Johann-Joachim-Becherweg 21, D-55128 Mainz, Germany

Now at Laboratoire des Sciences de l'Environnement Marin, UMR 6539, Institut Universitaire Européen de la Mer, Université de Bretagne Occidentale, IRD, CNRS, Technopole Brest-Iroise, Place Nicolas Copernic, F-29280 Plouzané, France (julien.thebault@univ-brest.fr)

Bernd R. Schöne and Nadine Hallmann

Earth System Science Research Centre Geocycles and INCREMENTS, Department of Applied and Analytical Paleontology, Institute of Geosciences, University of Mainz, Johann-Joachim-Becherweg 21, D-55128 Mainz, Germany

Matthias Barth

Earth System Science Research Centre Geocycles and Department of Geochemical Petrology, Institute of Geosciences, University of Mainz, Johann-Joachim-Becherweg 21, D-55128 Mainz, Germany

Elizabeth V. Nunn

Earth System Science Research Centre Geocycles and INCREMENTS, Department of Applied and Analytical Paleontology, Institute of Geosciences, University of Mainz, Johann-Joachim-Becherweg 21, D-55128 Mainz, Germany

[1] Interannual and intra-annual variations in lithium-to-calcium ratio were investigated with high temporal resolution in the aragonitic outer shell layer of juvenile *Arctica islandica* (Mollusca; Bivalvia) collected alive in 2006 off northeast Iceland. $\text{Li}/\text{Ca}_{\text{shell}}$ ranged between 7.00 and 11.12 $\mu\text{mol mol}^{-1}$ and presented well-marked seasonal cycles with minimum values recorded at the annual growth lines; a general pattern was a progressive increase in $\text{Li}/\text{Ca}_{\text{shell}}$ from March to May, followed by a plateau in June and a decrease down to minimum values in July–August. $\text{Li}/\text{Ca}_{\text{shell}}$ was correlated with $\delta^{18}\text{O}_{\text{shell}}$ -derived temperature, but the strength of this relationship was weak ($r^2 < 0.25$ and $p < 0.05$). It covaried significantly with microgrowth increment width and with the discharge from one of the closest rivers. Seasonal variations of $\text{Li}/\text{Ca}_{\text{shell}}$ in *A. islandica* may most likely be explained (1) by calcification rate and/or (2) by significant river inputs of Li-rich silicate particles flowing to the sea as soon as snow melts. In the first case, $\text{Li}/\text{Ca}_{\text{shell}}$ may be a useful proxy for addressing seasonal variations of growth rate in bivalves that lack discernable microgrowth patterns. Abrupt decreases of $\text{Li}/\text{Ca}_{\text{shell}}$ may, in turn, help identify growth retardations due to harsh environmental conditions. Alternatively, if $\text{Li}/\text{Ca}_{\text{shell}}$ variations are linked to particulate Li inputs by rivers, this could be a new proxy for the intensity of mechanical weathering of Icelandic basalts, with interesting perspectives for the reconstruction of frequency and intensity of past jökulhlaups (subglacial outburst floods). Further works, including experimental studies, are needed to test these hypotheses.

Components: 9851 words, 6 figures, 3 tables.

Keywords: bivalve; lithium; calcification; shell growth rate; weathering; Iceland.



Index Terms: 0424 Biogeosciences: Biosignatures and proxies; 0438 Biogeosciences: Diel, seasonal, and annual cycles (4227); 0454 Biogeosciences: Isotopic composition and chemistry (1041, 4870).

Received 19 August 2009; **Revised** 12 October 2009; **Accepted** 20 October 2009; **Published** 15 December 2009.

Thébault, J., B. R. Schöne, N. Hallmann, M. Barth, and E. V. Nunn (2009), Investigation of Li/Ca variations in aragonitic shells of the ocean quahog *Arctica islandica*, northeast Iceland, *Geochem. Geophys. Geosyst.*, 10, Q12008, doi:10.1029/2009GC002789.

1. Introduction

[2] During the past sixty years, a large number of studies have focused on the use of elemental concentrations in marine sediment cores as proxies for past variations of environmental parameters. These parameters include, among others, temperature (proxies: Mg/Ca, Sr/Ca), alkalinity (Ba/Ca), dissolved inorganic carbon concentration (Cd/Ca), ocean circulation (Cd/Ca, Nd, Hf, Pb), biological productivity (Ba/SO₄, Pa/Th, Be/Th, U) and sedimentation rate (²³⁰Th, ²¹⁰Pb, ²³¹Pa/²³⁰Th) (for thorough reviews, see *Wefer et al.* [1999] and *Henderson* [2002]). However, the temporal resolution of such paleoceanographic reconstructions is low, generally coarser than decades. Therefore, efforts have been made to assess the potential of elemental content in marine biogenic carbonates, especially bivalve mollusk shells, as high-resolution proxies for environmental conditions [e.g., *Stecher et al.*, 1996; *Vander Putten et al.*, 2000; *Thébault et al.*, 2009].

[3] Bivalve shells grow by accretion of calcium carbonate crystals, either in the form of calcite, aragonite, or both depending on the species [*Pannella and McClintock*, 1968]. Shell growth, however, does not occur continuously over a day, or over a year; instead, growth ceases periodically, on ultradian (several growth stops during a single day), circatidal (semidiurnal, ~12.4 h), circadian (solar day, ~24 h), circalunidian (lunar day, ~24.8 h), or annual time scales [*Schöne*, 2008]. These growth stops result in the formation of so-called growth lines, which are enriched in organic matter and separate growth increments that represent equal time slices. These periodic growth lines can therefore be used to assign precise calendar dates to each successive increment of accreted shell material. This characteristic gives bivalve shells an outstanding potential for the high-resolution reconstruction of paleoenvironmental conditions, especially through geochemical analyses. For example, skeletal oxygen isotope composition ($\delta^{18}\text{O}$) of many bivalve species (including scallops, mussels, and clams)

has been extensively used since the pioneering work of *Epstein et al.* [1953] to infer paleotemperature variations, sometimes with an accuracy of less than 1°C [*Chauvaud et al.*, 2005; *Thébault et al.*, 2007].

[4] In the past decade, the elemental composition of bivalve shells has also been increasingly used for paleoenvironmental reconstructions. Bivalve shells are not exclusively made of CaCO₃. Aside from Ca, a number of minor and trace elements are also incorporated within the shell during its formation, either in an interstitial location within the crystal lattice or as carbonates (substitution for Ca²⁺ [*Okumura and Kitano*, 1986]), or even within the organic matrix [*Lingard et al.*, 1992], which can represent up to 5% of the shell dry weight [*Marin and Luquet*, 2004]. The incorporation of these elements is known to be partly controlled by various environmental parameters, either physical (temperature, salinity), chemical (seawater elemental concentration, metallic contamination), or biological (primary production). Physiology, however, also exerts an important control on the chemical composition of bivalve shells [*Schöne*, 2008].

[5] Microanalytical techniques (e.g., laser ablation coupled to an ICP-MS system = LA-ICP-MS [*Craig et al.*, 2000]) allow the accurate measurement of tens of elements archived in biogenic carbonates within a few seconds. Their abiding improvement considerably increases the probability of discovering new paleoenvironmental proxies. With the exception of a few studies [e.g., *Lindh et al.*, 1988; *Carriker et al.*, 1996; *Dick et al.*, 2007] however, most investigations on the geochemical composition of bivalve shells have only dealt with a few elements (mainly Sr, Mg, Ba, and some trace metals including Mn, Pb, Zn, and Cd).

[6] Lithium is a trace element that (1) is easily measurable using mass spectrometers, (2) has been demonstrated to present an interesting potential as a paleoceanographic proxy in some marine biogenic carbonates [*Delaney et al.*, 1985, 1989; *Hall and Chan*, 2004; *Marriott et al.*, 2004a, 2004b;

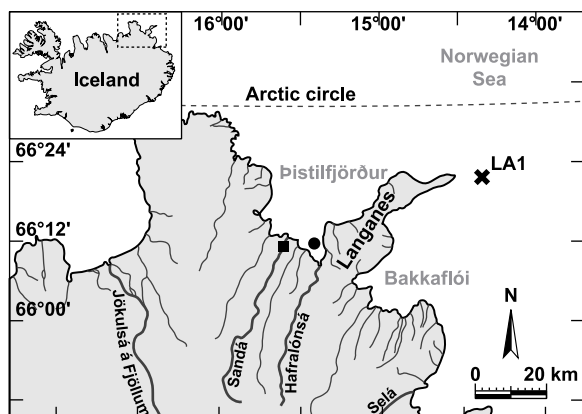


Figure 1. Map of northeastern Iceland showing Langes Peninsula between Þistilfjörður and Bakkafloi. *Arctica islandica* specimens were collected by dredging in Þistilfjörður at 30 m water depth (black dot). Temperature and salinity data used in this paper were measured off Langes Peninsula by the Marine Research Institute of Reykjavik (CTD station LA1, 20 m water depth, black cross). Seasonality of freshwater inputs in Þistilfjörður were assessed using river discharge data collected at Sandá River gauging station (black square).

Hathorne and James, 2006; Montagna et al., 2006], and (3) has surprisingly not yet been analyzed in bivalve shells. One of the first studies dealing with Li/Ca ratios in marine biogenic carbonates suggested that this ratio in foraminiferal calcite was partly controlled by the Li/Ca ratio of the growing medium [Delaney et al., 1985]. This was later confirmed by Hathorne and James [2006] who demonstrated that Li/Ca in foraminifera could be used to reconstruct past changes in the Li/Ca ratio of seawater, which could be interpreted in terms of continental silicate weathering rate. Several studies have also highlighted significant inverse relationships between temperature and Li/Ca in foraminifera [Hall and Chan, 2004; Marriott et al., 2004a], in calcitic brachiopods [Delaney et al., 1989], in coralline aragonite [Marriott et al., 2004b; Montagna et al., 2006], and in inorganic calcite [Marriott et al., 2004b]. It has finally been suggested that the main factor controlling Li incorporation in foraminifera is not temperature but calcification rate [Hall and Chan, 2004; Marriott et al., 2004a]. Because calcification rate may be a function of CO_3^{2-} concentration in the oceans, it has been suggested that the Li/Ca ratio in foraminifera could be a potential proxy of past atmospheric CO_2 [Hall and Chan, 2004].

[7] Here, we present for the first time Li/Ca records in bivalve mollusk shells. We have focused on juvenile ocean quahogs *Arctica islandica* (Linnaeus, 1767) collected alive in 2006 off the coast of northeast Iceland, probably one of the last pristine ecosystems in the North Atlantic. *A. islandica* has all the characteristics necessary for paleoceanographic reconstructions. First, it produces circadian and annual growth patterns in its aragonitic shell [Schöne et al., 2005a]. Second, it holds the longevity record for bivalves and may in fact be the longest-lived noncolonial animal, living up to 4 centuries [Schöne et al., 2005b; Wanamaker et al., 2008a]. Third, it exhibits a broad biogeographic distribution centered around Iceland, inhabiting the continental shelves on both sides of the North Atlantic, in Europe from the Barents Sea to the Bay of Cadiz in Spain, and in North America from Newfoundland to Cape Hatteras [Thorarinsdóttir and Jacobson, 2005]. Fourth, this species has been intensively studied for its anatomy, behavior, physiology, biology, and ecology [Witbaard, 1997]. And finally, several studies have already highlighted that shells of *A. islandica* provide multiproxy records of environmental variables. Changes in environmental parameters are recorded in variations of growth rates [Marchitto et al., 2000; Schöne et al., 2003, 2005b], stable isotope composition [Weidman et al., 1994; Schöne et al., 2004, 2005a, 2005b, 2005c; Wanamaker et al., 2008b] and trace element concentrations [Eplé, 2004; Toland et al., 2000; Liehr et al., 2005].

[8] The aims of this paper are (1) to analyze the behavior of Li/Ca in *A. islandica* aragonitic shells (interannual and intra-annual variability) using variations of the oxygen isotope composition of these shells as chronological checks, (2) to review the different processes that may explain the temporal variations of this ratio, and (3) to assess if Li/Ca could be a promising addition to the arsenal of proxies already used in bivalve shells.

2. Materials and Methods

2.1. Study Area

[9] Our study site is located in Þistilfjörður (northeast Iceland; $66^{\circ}10.751'N$, $15^{\circ}21.296'W$), 1 km off the southwestern edge of Langes Peninsula and 3 km away from Hafnalónsa estuary (Figure 1). Hafnalónsa and Sandá are the two main rivers flowing into Þistilfjörður. Catchments of these

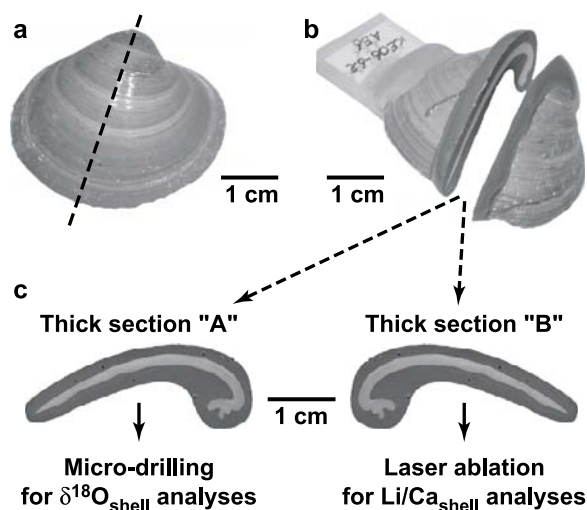


Figure 2. Preparation of *Arctica islandica* shells for geochemical analyses. (a) Right valve of *Arctica islandica*. The axis of maximum growth was identified on shells as the largest distance between the umbo and the ventral margin (dashed line). (b) After mounting on a Plexiglas cube and embedding in metal-epoxy resin, left valves were cut along the axis of maximum growth using a low-speed saw. (c) Two “mirroring” sections were cut in each shell, one for isotopic analyses (thick section “A”) and the other one for Li/Ca determination (thick section “B”).

two nonglacial rivers are composed of old basaltic rocks (>3.1 million years of age). Water depth at our study site is 30 m and the substrate mainly consists of sand and silt sediments. Hydrographic conditions off north Iceland largely depend on the physical characteristics of the East Icelandic Current, which, in turn, depend on the eastward transport of Greenland Polar Water by the East Greenland Current and the northward transport of Irminger Atlantic Water by the North Irminger Current [Hopkins, 1991]. No environmental survey has ever been conducted in Þistilfjörður because of its isolated situation in this remote part of Iceland. The closest site where environmental data are available is located 50 km northeastward of our study site, off the northeastern part of the Langanes Peninsula (Langanes Austur LA1, 66°22'N, 14°22'W (Figure 1)). Environmental conditions at LA1 are also mainly controlled by the relative intensities of the East Icelandic Current and the North Irminger Current. Temperature and salinity are measured at this location at a depth of 20 m by the Oceanographic Group of the Marine Research Institute of Reykjavik using a CTD profiler (data available at <http://www.hafro.is/Sjora/>). This data set indicates that water temperature is lowest in

February–March (mean [2000–2006] = 2.8°C; σ = 0.9°C) and reaches a maximum in August (7.9°C; σ = 0.8°C). Over the same period, salinity variations ranged between 34.4 and 34.8. These temperature and salinity values are similar to those measured at 20–30 m water depth in two other fjords in North Iceland: Reykjarfjörður [Andrews *et al.*, 2001] and Ísafjörður [Astthorsson, 1990]. From early May to the end of August, somewhat lower salinities (<34) can be observed near the surface in Icelandic fjords because of meltwater runoff from the land. However, these low salinities are restricted to the top 10 m of the water column [Astthorsson, 1990; Andrews *et al.*, 2001]. Therefore, temperature and salinity data measured at 20 m depth at LA1 likely reflect those of our study site at 30 m depth.

[10] The seawater oxygen isotope composition of our study site was measured on 17 August 2006 ($\delta^{18}\text{O}_{\text{water}} = -0.58\text{‰}$ VSMOW; Salinity = 34.58). Seasonal variations in $\delta^{18}\text{O}_{\text{water}}$ are expected given the salinity variations around the Langanes Peninsula but coefficients of the local $\delta^{18}\text{O}_{\text{water}}$ –salinity relationship are unknown. The $\delta^{18}\text{O}_{\text{water}}$ and salinity values were measured off northwest Iceland in October 1998 (65.98–68.72°N; 22.98–29.25°W; depth = 10–30 m) in the framework of the VEINS Program (Variability of Exchanges In the Northern Seas; data compiled by Schmidt *et al.* [1999]). These data indicate that, over the salinity range 32–35, we can expect a lowering of the $\delta^{18}\text{O}_{\text{water}}$ values of 0.68‰ for every unit decrease in salinity. Given (1) $\delta^{18}\text{O}_{\text{water}}$ and salinity values measured on 17 August 2006 at our study site and (2) the slope of the $\delta^{18}\text{O}_{\text{water}}$ –salinity relationship derived from the VEINS Program, we can expect seasonal variations of $\delta^{18}\text{O}_{\text{water}}$ at our study site of between –0.7 and –0.4‰ VSMOW over the salinity range 34.4–34.8.

2.2. Shell Sampling and Preparation

[11] Two specimens of *Arctica islandica* were collected alive on 17 August 2006 by dredging on our study site in Þistilfjörður, at a depth of 30 m. Both specimens (ICE06–6.2-A55 and ICE06–6.2-A56, hereafter simply named A55 and A56) were juveniles with a shell height of 33.0 and 31.2 mm, respectively (shell length of 40.0 and 37.4 mm, respectively (Figure 2a)). We chose young specimens because *A. islandica* grows fairly rapidly during early ontogenetic stages [Jones, 1983; Weidman *et al.*, 1994; Jones, 1998; Kilada *et al.*, 2007] and young shells



therefore provide the highest temporal resolution in carbonate records.

[12] Immediately after dredging, the soft parts were discarded and the right and left valves kept frozen until analysis. The left valves of shells A55 and A56 were gently rinsed with deionized water and air dried. Each valve was mounted on a Plexiglas cube using a two-part methacrylate glue (plastic welder, Gluetec GmbH and Co. KG, Germany) and embedded in a two-part metal-epoxy resin (Wiko, Germany) to strengthen the shell and to avoid shell fracture during sawing (Figure 2b). Two immediately adjacent, 2.6 mm thick sections were cut from each valve perpendicular to the growth lines along the axis of maximum growth using a low-speed precision saw (Isomet 1000, Buehler Ltd., Illinois, United States) equipped with a 0.4 mm thick diamond-coated blade cooled and kept wet using deionized water (Figure 2c). These “mirroring” sections were then mounted on glass slides, manually ground with $\sim 12 \mu\text{m}$ and $8 \mu\text{m}$ SiC powder, and polished with $1 \mu\text{m}$ Al_2O_3 powder to visualize the internal growth patterns. Thick sections were ultrasonically rinsed with deionized water between each grinding/polishing step to remove any adhering grinding powder. Thick section “A” was used for isotopic analyses and thick section “B” for trace elemental analyses. Once geochemical analyses were done, these thick sections were cleaned with ethanol before being etched in the so-called Mutvei’s solution for 25 min at $37\text{--}40^\circ\text{C}$ in order to resolve interannual and intra-annual growth lines and increments (see *Schöne et al.* [2005d] for a detailed description of this method). Finally, the sections were gently rinsed with deionized water and air dried. Micro-growth increment width was subsequently measured using the image analysis software Panopea (© 2004 Peinl and Schöne). High-resolution photographs of these four sections were taken using a Nikon Coolpix 995 digital camera attached to a Wild Heerbrugg M3Z stereozoom microscope. Photo stitching software (Photoshop Elements 2.0) was then used to assemble the 25–30 photographs taken for each section into a single, high-resolution picture.

2.3. Isotopic Analyses

[13] The oxygen isotope ratio ($^{18}\text{O}/^{16}\text{O}$) of marine biogenic carbonate is controlled by temperature and the oxygen isotope composition of the seawater from which it precipitates [*McCrea*, 1950; *Epstein et al.*, 1953]. Therefore, shells of our two

A. islandica specimens were sampled for isotopic analyses in order to reconstruct variations in the bottom water temperatures these animals experienced during their life. Aragonite samples (48 and 50 samples on shells A55 and A56, respectively) were collected in thick sections “A” using a micro-drill (Minimo C121, Minitor Co. Ltd., Japan) equipped with a 0.3 mm tungsten carbide drill bit (model H52.104.003, Gebr. Brasseler GmbH and Co. KG, Germany). Samples were taken in the outer shell layer along an axis running from the ventral margin and toward the youth portions of the shells. Holes drilled in these sections were $\sim 350 \mu\text{m}$ in diameter. Aliquots of shell aragonite weighing between 38 and $125 \mu\text{g}$ (mean = $80 \mu\text{g}$) were analyzed at the University of Frankfurt using an automated Gas Bench II carbonate device interfaced with a Thermo Finnigan MAT 253 isotope ratio mass spectrometer. Shell isotopic data are expressed in conventional delta (δ) notation [*Epstein et al.*, 1953] relative to the VPDB standard. The in-house standard used was a Carrara marble ($\delta^{18}\text{O}_{\text{Carrara}} = -1.74\text{‰}$ VPDB) calibrated against NBS19. The isotopic value used for this calibration was $\delta^{18}\text{O}_{\text{NBS19}} = -2.20\text{‰}$ VPDB (for more details, see *Fiebig et al.* [2005]). Repeated analyses of this standard yielded a reproducibility (1σ) of 0.07‰ VPDB.

[14] To temporally align aragonite samples taken between two annual growth lines, we compared the temperature reconstructed from our $\delta^{18}\text{O}_{\text{shell}}$ records (hereafter referred as $T_{\delta^{18}\text{O}}$) with seasonal variations of seawater temperature measured at 20 m depth at station LA1. To this end, we used the empirically determined paleothermometry equation of *Grossman and Ku* [1986, equation 1]. A modification of this equation was, however, required as their water values were reported in VSMOW minus 0.27‰ [*Hut*, 1987]. Once corrected, their equation translates to:

$$T_{\delta^{18}\text{O}} = 19.43 - 4.34(\delta^{18}\text{O}_{\text{shell}} - \delta^{18}\text{O}_{\text{water}}) \quad (1)$$

where $T_{\delta^{18}\text{O}}$ is seawater temperature (in $^\circ\text{C}$) reconstructed from $\delta^{18}\text{O}_{\text{shell}}$, and $\delta^{18}\text{O}_{\text{shell}}$ and $\delta^{18}\text{O}_{\text{water}}$ are the oxygen isotope composition of aragonite and water expressed in ‰ relative to the VPDB and VSMOW standards, respectively. We used an average $\delta^{18}\text{O}_{\text{water}}$ value of -0.55‰ VSMOW. In order to estimate the uncertainty on $T_{\delta^{18}\text{O}}$, i.e., half the difference between upper and lower bounds, we applied the following formula using (1) the uncertainty in $\delta^{18}\text{O}_{\text{shell}}$ value given by

Table 1. LA-ICP-MS Operating Conditions

Parameter	Value
<i>Laser: New Wave Research UP-213</i>	
Crystal	Nd:YAG
Wavelength	213 nm
Laser mode	Q-switched
Laser power	0.2 mJ
Repetition rate	10 Hz
Pit diameter	80 μm
Ablation time	60 s
Background	60 s
<i>ICP-MS: Agilent 7500ce</i>	
RF power	1200 W
Plasma gas flow	15 L min^{-1}
Auxiliary gas flow	1 L min^{-1}
Carrier gas flow	0.65 L min^{-1}
Optional gas flow	75% He
Acquisition mode	pulse counting
Acquisition time	120 s
Dwell time	10 ms

IR-MS ($\varepsilon_{\text{IRMS}} = \pm 0.07\text{‰}$) and (2) the estimated range of $\delta^{18}\text{O}_{\text{water}}$ (min. = -0.7‰ ; max. = -0.4‰):

$$\text{Uncertainty} = 4.34 \times (2\varepsilon_{\text{IRMS}} + \delta^{18}\text{O}_{\text{water max.}} - \delta^{18}\text{O}_{\text{water min.}}) / 2 \quad (2)$$

This resulted in an absolute uncertainty on $T_{\delta^{18}\text{O}}$ of $\pm 0.95^\circ\text{C}$.

2.4. Li/Ca_{shell} Analyses

[15] Li/Ca ratios were analyzed in thick sections “B” using LA-ICP-MS at the University of Mainz. An Agilent 7500ce quadrupole ICP-MS (Agilent Technologies Inc., California, United States) coupled to a UP-213 laser ablation system (New Wave Research, California, United States) was used with the parameters listed in Table 1. Aragonite samples ($n = 332$ in each shell) were ablated in the outer shell layer from the ventral margin toward the youth portions of the shells at a constant distance from the shell surface ($400 \mu\text{m}$). The diameter of the laser spots was $80 \mu\text{m}$ and the distance between the centers of two successive spots was $100 \mu\text{m}$ (i.e., $20 \mu\text{m}$ between edges of two successive spots). During acquisition, signal intensities were recorded for ^7Li , ^{43}Ca and ^{44}Ca . The intensity of the isotope of interest was systematically normalized against the ^{43}Ca signal (internal standard) in order to correct for laser beam energy drift, focus variation at the sample surface, and ICP-MS detection drift [see Pearce *et al.*, 1997]. The glass

reference material NIST SRM 612 was used as a calibration standard with the values of Pearce *et al.* [1997]. Precision (degree of reproducibility) and accuracy (degree of veracity) of the applied method were controlled by repeated analyses of the glass reference material NIST SRM 614 (Li concentration value taken from Kurosawa *et al.* [2002]). For each shell, the sequence of analyses was as follows: (NIST612) \times_2 + shell \times_2 + (shell \times_{15} + NIST614 + shell \times_{15} + NIST612) \times_{11} + NIST612. Data processing (including instrumental drift correction and normalization) was performed using GLITTER v.4 software (Macquarie Research Ltd., Australia [Van Achterbergh *et al.*, 2001]), following the methods of Longerich *et al.* [1996].

[16] Li/Ca detection limit at the 99% confidence level was calculated by GLITTER using Poisson counting statistics and was $0.243 \mu\text{mol mol}^{-1}$. Repeated measurements of NIST SRM 614 ($n = 22$) yielded a precision of 1.9% (% RSD). Accuracy was extremely good with a Li concentration value in NIST SRM 614 of $1.687 \pm 0.007 \mu\text{g g}^{-1}$ compared with the recommended value of $1.69 \pm 0.026 \mu\text{g g}^{-1}$ (means \pm standard errors).

2.5. Statistical Analyses

[17] Two different statistical tests were used to compare the means of two independent samples: Student’s t test (large samples: $\min(n_1, n_2) \geq 30$) and Mann-Whitney U test (small samples: $\min(n_1, n_2) < 30$). An analysis of covariance (ANCOVA; $\alpha = 0.05$) was used to test whether there were significant differences between the slopes of the least squares linear regressions (Li/Ca_{shell} versus $T_{\delta^{18}\text{O}}$) calculated for each of the two shells. Homogeneity of residual variances was tested with Bartlett’s test ($\alpha = 0.01$). No data were excluded. All statistical analyses were performed according to Scherrer [1984].

3. Results

3.1. Profiles of $\delta^{18}\text{O}_{\text{shell}}$

[18] In each shell, $\delta^{18}\text{O}_{\text{shell}}$ profile showed cyclical oscillations in phase with the main growth lines that were revealed after the immersion of shell sections in Mutvei’s solution (Figure 3). This confirms the annual periodicity of these growth lines. Seven main growth lines were observed in both shells, suggesting that both specimens settled on the seafloor in 1999. Isotopic data covered four full years of growth (2002–2005) and the beginning of year 2006.

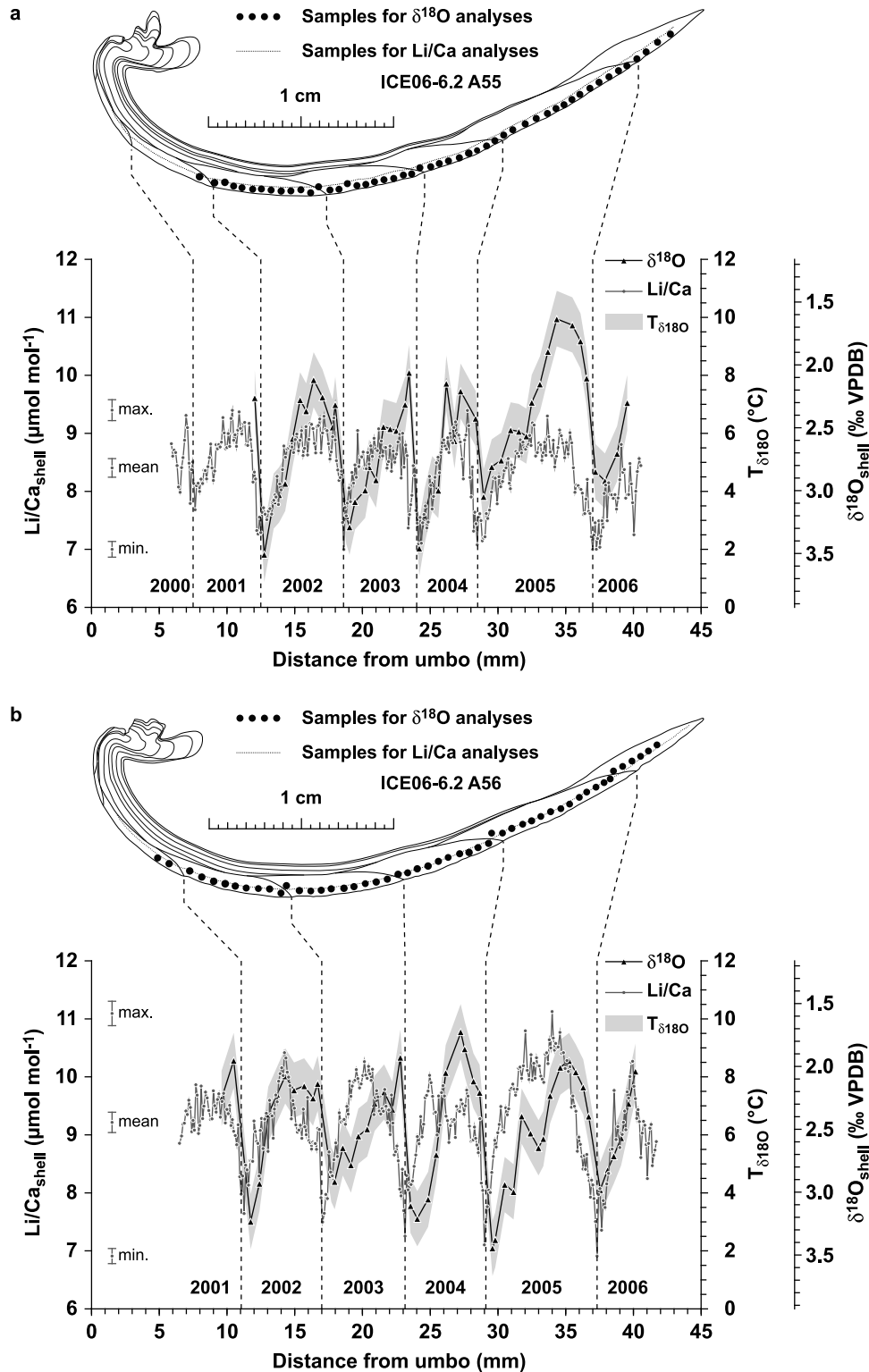


Figure 3. Temporal variations (2000–2006) of Li/Ca_{shell} ratio (gray circles), $\delta^{18}\text{O}_{\text{shell}}$ (black triangles; inverted scale), and $\delta^{18}\text{O}_{\text{shell}}$ -derived seawater temperature ($T_{\delta^{18}\text{O}}$, gray area) measured in *Arctica islandica* shells. (a) Specimen A55. (b) Specimen A56. Error bars on the left side of each plot correspond to Li/Ca_{min.} \pm 1RSD, Li/Ca_{mean} \pm 1RSD, and Li/Ca_{max.} \pm 1RSD, with RSD = 1.9% (precision given by 22 measurements of NIST SRM 614). Vertical dashed lines represent the annual growth lines revealed in shell cross sections and are used to identify the different years of growth. Also presented are digitized cross sections of the two specimens, showing annual growth lines in outer and inner shell layers, and location of aragonite samples taken for isotopic and elemental analyses.

Table 2. Annual Amplitudes of $\delta^{18}\text{O}_{\text{shell}}$ and $T_{\delta^{18}\text{O}}$ of Specimens A55 and A56 Over the Period 2002–2006^a

Year	Shell	$\delta^{18}\text{O}_{\text{shell}}$ (‰VPDB)		$T_{\delta^{18}\text{O}}$ ($\pm 0.95^\circ\text{C}$)	
		Minimum	Maximum	Minimum	Maximum
2002	A55	2.12	3.51	1.8	7.8
	A56	2.08	3.23	3.0	8.0
2003	A55	2.06	3.29	2.8	8.1
	A56	1.93	2.92	4.4	8.7
2004	A55	2.15	3.46	2.0	7.7
	A56	1.73	3.21	3.1	9.5
2005	A55	1.64	3.05	3.8	9.9
	A56	1.96	3.45	2.1	8.5
2006	A55	–	2.92	4.4	–
	A56	–	2.98	4.1	–

^a $T_{\delta^{18}\text{O}}$ were calculated using equation (1) using a mean $\delta^{18}\text{O}_{\text{water}}$ value of -0.55‰ . The uncertainty in temperature reconstruction from $\delta^{18}\text{O}_{\text{shell}}$ is $\pm 0.95^\circ\text{C}$.

[19] $\delta^{18}\text{O}_{\text{shell}}$ values ranged from 1.64 to 3.51‰ in shell A55 and from 1.73 to 3.45‰ in shell A56. Annual minima ranged from 1.64 to 2.15‰, whereas annual maxima varied between 2.92 and 3.51‰ (Table 2). Seasonal $\delta^{18}\text{O}_{\text{shell}}$ cycles were strongly right skewed with minimum/maximum values occurring shortly before/after the annual growth lines (Figure 3).

[20] These $\delta^{18}\text{O}_{\text{shell}}$ values were converted into temperature ($T_{\delta^{18}\text{O}}$) using equation (1) and a $\delta^{18}\text{O}_{\text{water}}$ value of -0.55‰ (Figure 3). Annual minimum temperatures recorded by the shells ranged from 1.8 to 4.4°C (mean [2002–2006] = 3.1°C; $\sigma = 1.0^\circ\text{C}$ (Table 2)). Mean annual minima in shells A55 (3.0°C) and A56 (3.3°C) were not significantly different from each other (Mann-Whitney $U = 8.5$, $n_1 = n_2 = 5$, $p > 0.05$). Annual maximum temperatures recorded by the shells ranged from 7.7 to 9.9°C (mean [2002–2005] = 8.5°C; $\sigma = 0.8^\circ\text{C}$ (Table 2)). Mean annual maxima in shells A55 (8.4°C) and A56 (8.7°C) did not differ significantly (Mann-Whitney $U = 5$, $n_1 = n_2 = 4$, $p > 0.05$).

[21] The offsets between $T_{\delta^{18}\text{O}}$ and T_{LA1} (0.3°C and 0.6°C for average annual minima and maxima, respectively) are within the $\pm 0.95^\circ\text{C}$ uncertainty on $T_{\delta^{18}\text{O}}$, so it is reasonable to assume that the whole annual range of seawater temperature was recorded by the shells.

3.2. Li/Ca_{shell} Profiles

[22] For both specimens, Li/Ca_{shell} profiles showed cyclical variations with minimum values recorded exactly at the annual growth lines (Figure 3). A general tendency of the seasonal Li/Ca_{shell} varia-

tions was a progressive increase after the annual line, followed by a plateau and then a decrease down to minimum values. Maximum Li/Ca_{shell} values tended to occur earlier during the growing season than $\delta^{18}\text{O}_{\text{shell}}$ minima (i.e., before temperature maxima (Figure 3)).

[23] Li/Ca_{shell} ranged from 7.00 to 9.40 $\mu\text{mol mol}^{-1}$ in shell A55 (mean = 8.37 $\mu\text{mol mol}^{-1}$ (Figure 3a)) and from 6.91 to 11.12 $\mu\text{mol mol}^{-1}$ in shell A56 (mean = 9.23 $\mu\text{mol mol}^{-1}$ (Figure 3b)). Mean Li/Ca_{shell} ratio was significantly higher in shell A56 than in shell A55 (t test $t = 16.87$, $n_1 = n_2 = 332$, $p < 0.01$).

[24] Annual minimum values ranged from 7.00 to 7.29 $\mu\text{mol mol}^{-1}$ in shell A55 (mean [2001–2005] = 7.16 $\mu\text{mol mol}^{-1}$; $\sigma = 0.12 \mu\text{mol mol}^{-1}$), and from 7.10 to 7.64 $\mu\text{mol mol}^{-1}$ in shell A56 (mean [2002–2005] = 7.44 $\mu\text{mol mol}^{-1}$; $\sigma = 0.23 \mu\text{mol mol}^{-1}$ (Table 3)). Mean annual minima in shells A55 and A56 did not differ significantly (Mann-Whitney $U = 3$, $n_1 = 5$, $n_2 = 4$, $p > 0.05$).

[25] Annual maxima ranged from 9.08 to 9.40 $\mu\text{mol mol}^{-1}$ in shell A55 (mean [2001–2005] = 9.30 $\mu\text{mol mol}^{-1}$; $\sigma = 0.13 \mu\text{mol mol}^{-1}$), and from 10.03 to 11.12 $\mu\text{mol mol}^{-1}$ in shell A56 (mean [2002–2005] = 10.46 $\mu\text{mol mol}^{-1}$; $\sigma = 0.22 \mu\text{mol mol}^{-1}$ (Table 3)). Mean annual maximum in shell A56 was significantly higher than in shell A55 (Mann-Whitney $U = 0$, $n_1 = 5$, $n_2 = 4$, $p < 0.05$).

[26] As a consequence, mean annual amplitude in shells A55 (2.14 $\mu\text{mol mol}^{-1}$) and A56 (3.02 $\mu\text{mol mol}^{-1}$) were significantly different (Mann-Whitney $U = 0$, $n_1 = 5$, $n_2 = 4$, $p < 0.05$). Annual amplitude ranged from 2.01 to 2.32 $\mu\text{mol mol}^{-1}$ in shell A55, and from 2.76 to 3.63 $\mu\text{mol mol}^{-1}$ in shell A56 (Table 3).

[27] Li/Ca_{shell} in both shells was statistically correlated with the $\delta^{18}\text{O}_{\text{shell}}$ -derived temperature ($p < 0.05$ for both specimens (Figure 4)). An ANCOVA showed no significant difference between slopes of the two linear regressions (Bartlett's test: $B_C = 5.52$, $df = 1$; ANCOVA: $F = 0.02$, $df = 1$ and 95). The strength of these correlations was, however, extremely weak with determination coefficients ranging from 0.11 (shell A56) to 0.25 (shell A55). The difference in intercept values ($\sim 1 \mu\text{mol mol}^{-1}$) reflects the difference in annual maxima between shell A56 and shell A55.

[28] The comparison of Li/Ca_{shell} variations with daily shell growth rates was difficult because we were unexpectedly unable to resolve microgrowth

Table 3. Annual Minima, Maxima, and Amplitude of Li/Ca_{shell} Values of Specimens A55 and A56 Over the Period 2001–2005

Year	Shell	Minimum Li/Ca _{shell}	Maximum Li/Ca _{shell}	Annual Amplitude
2001	A55	7.26	9.40	2.13
	A56	–	–	–
2002	A55	7.29	9.29	2.01
	A56	7.64	10.42	2.77
2003	A55	7.00	9.08	2.08
	A56	7.50	10.26	2.76
2004	A55	7.08	9.39	2.32
	A56	7.10	10.03	2.92
2005	A55	7.15	9.30	2.15
	A56	7.50	11.12	3.63

structures over the whole shell sections despite etching with Mutvei's solution. Nevertheless, 22 groups of 3–5 microgrowth increments were quite clearly revealed in the A56 shell portion formed in 2004. The average increment width in each of these 22 batches was calculated and plotted with the A56 Li/Ca_{shell} record for year 2004 (Figure 5a). Although the number of increment data was limited, our data showed that Li/Ca_{shell} covaried with microgrowth increment width, which ranged from 24 to 28 μm near the annual lines to 43 μm in the first half of the 2004 growing season (average = 32.3 μm). A simple linear regression indicated that microgrowth increment width explained 53% of the Li/Ca_{shell} variability in shell A56 ($p < 0.001$ (Figure 5b)). Note that all geochemical and shell growth data obtained on specimens A55 and A56 can be retrieved in the auxiliary material.¹

4. Discussion

4.1. Seasonal Timing of Geochemical Records in Shells

[29] The present study is the first to investigate Li/Ca records in bivalve shells. Li/Ca_{shell} seasonal variations in our two *Arctica islandica* specimens were well marked, presenting a 1.3- to 1.6-fold range over a given growing season (Figure 3). The interannual variability between ontogenetic ages 3 to 8 was far less pronounced than intra-annual variability. Combined analyses of Li/Ca_{shell} and $\delta^{18}\text{O}_{\text{shell}}$, and reconstruction of seawater temperature from $\delta^{18}\text{O}_{\text{shell}}$ allowed us to estimate the seasonal timing of Li/Ca_{shell} variations.

[30] $T_{\delta^{18}\text{O}}$ variations (average annual range = 3.1–8.5°C) showed that the whole annual range of seawater temperature (2.8 to 7.9°C at 20 m depth at LA1) was recorded by the shells (Table 2). This implies that *A. islandica* shells did not stop growing because of thermal stress. Conversely, the position of the annual growth breaks between minimum and maximum $\delta^{18}\text{O}_{\text{shell}}$ (i.e., between maximum and minimum temperatures, recorded in August and March, respectively) suggests that shells stopped growing between September and February. The average microgrowth increment width measured in shell A56 was 32.3 μm at ontogenetic age 6, i.e., similar to the value calculated by Schöne *et al.* [2005a] for North Sea specimens (31.5 μm at ontogenetic age 4). This suggests that shell growth lasted ~ 185 days to achieve the 5.96 mm width of the 2004 annual increment. This result supports the hypothesis of an ~ 6 month growth break between September and February. As minimum temperatures were recorded by $\delta^{18}\text{O}_{\text{shell}}$, shells did not stop growing because of harsh winter conditions. Schöne *et al.* [2005a] showed that *A. islandica* specimens from the North Sea stopped growing from early September to mid-November and described this growth break as a spawning biocheck. In Iceland, *A. islandica* spawning activity peaks in June–July, whereas gametogenesis occurs from January to May [Thorarinsdóttir, 2000]. Therefore, the annual growth breaks found in our specimens cannot be attributed to reproductive activity. Moreover, our specimens were likely juveniles as in Icelandic waters, only 10% of *A. islandica* of 40 mm shell length are mature [Thorarinsdóttir and Jacobson, 2005]. Therefore, the origin of these annual growth breaks remains unclear. Their investigation, however, is far beyond the goals of this paper. The most important point is that the timing of the growing season determined by $T_{\delta^{18}\text{O}}$ variations allowed us to conclude that Li/Ca_{shell} increases from March to May, i.e., right after the annual line, stays roughly stable in June, and then decreases in July–August.

4.2. Processes Potentially Involved in Li/Ca_{shell} Seasonal Variations

[31] The shape of Li/Ca_{shell} variations is very similar in shells A55 and A56 and as such this ratio likely responds to environmental variations or to variations of a physiological process synchronized within a given population by genetic and/or exogenous factors. Based on published literature on Li/Ca ratios in CaCO₃ structures, the following

¹Auxiliary materials are available at <ftp://ftp.agu.org/apend/gc/2009gc002789>.

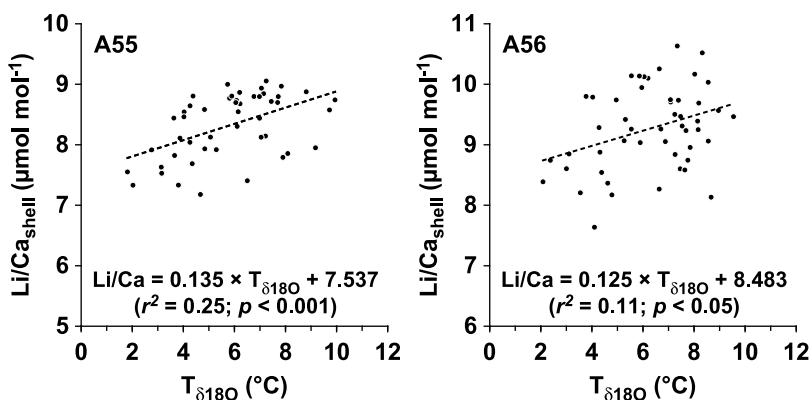


Figure 4. Correlations between $\delta^{18}\text{O}_{\text{shell}}$ -derived seawater temperature ($T_{\delta^{18}\text{O}}$) and Li/Ca_{shell} ratio in shells A55 ($n = 48$) and A56 ($n = 50$).

parameters may provide plausible hypotheses to explain the Li/Ca_{shell} variations in *A. islandica*: temperature, calcification rate, and Li/Ca ratio in seawater. Their potential influence on the shell geochemistry will be discussed in light of the evidence presented here. A fourth hypothesis will also be put forward: the influence of suspended Li-rich particles originating from the mechanical weathering of basaltic rocks.

4.2.1. Temperature

[32] Several studies have found a significant inverse relationship between Li/Ca in CaCO_3 structures and temperature in coralline aragonite [Marriott *et al.*, 2004b; Montagna *et al.*, 2006], in foraminiferal calcite [Hall and Chan, 2004; Marriott *et al.*, 2004a], in calcitic brachiopods [Delaney *et al.*, 1989], and in inorganic calcite [Marriott *et al.*, 2004b]. We also found relationships with temperature in *A. islandica* aragonitic shells but these were positive, not negative (Figure 4). Unlike these previous studies, our findings agree with thermodynamic calculations predicting that Li concentration in CaCO_3 structures should decrease with decreasing temperature [Hall and Chan, 2004]. According to Okumura and Kitano [1986], Li is incorporated in the crystal structure of aragonite in substitution of Ca, leading to the formation of lithium carbonate (Li_2CO_3) crystals. Smith *et al.* [1971] showed that the solubility of Li_2CO_3 increases with decreasing temperature. In other words, crystallization of Li_2CO_3 becomes easier as temperature rises (an almost linear relationship between 0 and 30°C [Smith *et al.*, 1971]). Although statistically significant ($p < 0.05$), the strength of our temperature-Li/Ca_{shell} relationships is extremely weak ($0.11 < r^2 < 0.25$). The weakness of this

relationship is particularly obvious for the 2003 Li/Ca_{shell} record in shell A56 where an important offset can be seen between Li/Ca_{shell} and $\delta^{18}\text{O}_{\text{shell}}$ (Figure 3b). Our findings suggest that if temperature-dependent solubility of Li_2CO_3 really plays a role on Li/Ca_{shell} in *A. islandica*, this influence is extremely weak.

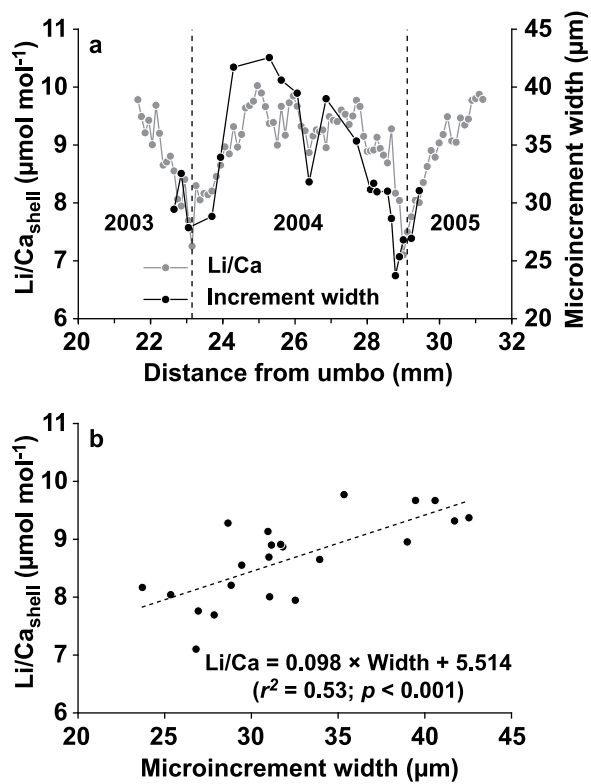


Figure 5. (a) Li/Ca_{shell} profile (gray circles) and microgrowth increment width (black circles) measured during the 2004 growing season in shell A56. (b) Simple linear regression performed between Li/Ca_{shell} and microgrowth increment width in shell A56 ($n = 22$).



4.2.2. Calcification Rate

[33] Many authors have suggested that the main factor controlling Li incorporation in foraminiferal calcite could be calcification rate, which may itself correlate partly with temperature [Delaney *et al.*, 1985; Hall and Chan, 2004; Marriott *et al.*, 2004a]. According to Carré *et al.* [2006], crystal growth rate strongly influences incorporation of Sr, Ba, Mn, and Mg in aragonitic shells of two Peruvian bivalve species (*Mesodesma donacium* and *Chione subrugosa*). However, they did not investigate Li/Ca_{shell} ratios. Our own results seem to support these findings. Indeed, we found a relatively strong relationship between microgrowth increment width and Li/Ca in *A. islandica* shells (Figure 5). Although microgrowth increment width represents the dorso-ventral linear extension of the shell per unit time and may slightly differ from the absolute calcification rate (see Gillikin *et al.* [2005] for elaboration), our results suggest that Li/Ca_{shell} may increase as a direct response of increasing calcification rate. Another argument in favor of this hypothesis is the difference observed in the range of Li/Ca variations in shells A55 and A56; although these two specimens appeared to have grown at an equivalent annual rate from 1999 to 2006, it can be assumed that A56 reached higher daily growth rates in summer than A55, explaining the difference in annual Li/Ca_{shell} maxima between these two shells. The mechanisms involved in these vital effects are unknown and any discussion on that subject would be highly speculative due to the scarcity of studies dealing with the formation of Li₂CO₃ crystals within aragonitic structures. Identification of these mechanisms would require biomineralization and/or inorganic precipitation experiments.

4.2.3. Li/Ca_{seawater}

[34] Delaney *et al.* [1985] and Hathorne and James [2006] suggested that Li/Ca ratio in calcitic foraminifera was directly controlled by the Li/Ca of the growing medium. Could possible variations of Li/Ca_{seawater} over *A. islandica* growing season have an influence on the shell geochemistry? Li is essentially conservative in seawater with an almost constant concentration of 26 μmol L⁻¹ and a Li/Ca_{seawater} ratio of ~2310 μmol mol⁻¹ [Li, 2000]. It has no significant involvement in biological activity or scavenging by particles [Stoffyn-Egli and Mackenzie, 1984]. Given the long residence times of Li (1.5 million years [Huh *et al.*, 1998]) and Ca (1 million years [Broecker and Peng, 1982]), the Li/Ca ratio of the global ocean has

probably not changed over the Holocene [Hall and Chan, 2004]. The two major sources of Li to the ocean are (1) high-temperature basalt-seawater reactions and (2) river input from the weathering of continental crust [Hoefs and Sywall, 1997]. In hydrothermal systems near the mid-ocean ridges, Li is leached from oceanic basalts at temperatures >250°C [Hoefs and Sywall, 1997]. Although the mid-Atlantic ridge runs right through Iceland, it is unlikely that such high temperatures could be reached at shallow coastal locations. Moreover, it is hardly conceivable that Li leaching from this ridge would follow a seasonal pattern; it is rather roughly constant throughout the year. Therefore, high-temperature hydrothermal circulation can certainly not explain Li/Ca_{shell} seasonal variations.

[35] Seasonal variations of riverine inputs may, however, have a local influence on Li/Ca ratios in coastal waters. Intensities of chemical and mechanical weathering of silicate rocks like basalts are usually expressed in terms of fluxes of dissolved and suspended materials, respectively [Gislason *et al.*, 2009]. Gislason *et al.* [2009] found a relationship between air temperature and chemical weathering rate in 8 northeastern Iceland river catchments. Air temperature in Iceland starts increasing in March and reaches maxima in July. Intensity of chemical weathering may therefore follow the same general pattern as Li/Ca_{shell}. Pogge von Strandmann *et al.* [2006] analyzed the chemical composition of 25 Icelandic rivers in September 2003 and August 2005 and found an average dissolved Li concentration of 87.5 nmol L⁻¹ (range: 1.54–1250 nmol L⁻¹) and a Li/Ca_{river} ratio ranging from 31 to 2461 μmol mol⁻¹ (average = 563 μmol mol⁻¹). This dissolved Li concentration range is similar to that measured by Vigier *et al.* [2009] in the major Icelandic rivers (range: 3–317 nmol L⁻¹; average = 86.5 nmol L⁻¹). These values may be slightly higher in July, i.e., at the annual air temperature maximum. According to Delaney *et al.* [1985], a 1.8- to 2.6-fold increase of the average Li/Ca_{seawater} ratio is necessary to observe a 1.3- to 1.6-fold increase of Li/Ca in calcitic foraminifera. This relationship can probably not be applied to *A. islandica* shells because of their aragonitic structure. Nevertheless, it highlights that Li/Ca_{seawater} must increase significantly to induce a 1.3- to 1.6-fold increase of Li/Ca in biogenic carbonates. Given that the maximum Li/Ca_{river} ratio measured by Pogge von Strandmann *et al.* [2006] was only 1.1-fold higher than Li/Ca_{seawater}, seasonal variations of basalt chemical weathering and dis-

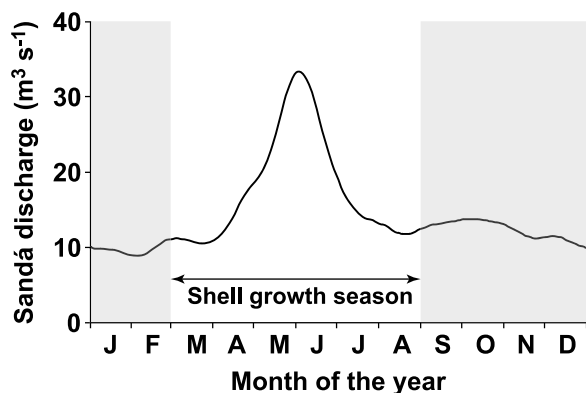


Figure 6. Long-term smoothed daily averages of Sandá River discharge (data obtained from the Hydrological Service of the Icelandic National Energy Authority). Maximum discharge is recorded in May and June, i.e., in the middle of *A. islandica* shell growth season.

solved Li flux can hardly explain the full variability of $\text{Li}/\text{Ca}_{\text{shell}}$ in *A. islandica*.

4.2.4. Suspended Li-Rich Basaltic Particles

[36] A fourth hypothesis could be put forward to explain $\text{Li}/\text{Ca}_{\text{shell}}$ seasonal variations: the possible influence of weathered basaltic particles carried by rivers. Seasonal variations of Sandá River discharge were obtained from the Hydrological Service of the Icelandic National Energy Authority (<http://www.os.is/>) (Figure 6). These data show that discharge roughly follows the same seasonal pattern as $\text{Li}/\text{Ca}_{\text{shell}}$, with values ranging from $\sim 10 \text{ m}^3 \text{ s}^{-1}$ in fall and winter to $\sim 35 \text{ m}^3 \text{ s}^{-1}$ in June (long-term average). Could these variations in river discharge induce large changes in the flux of suspended particles? Gislason *et al.* [2009] described and quantified a direct relationship between river discharge and mechanical weathering (expressed as suspended inorganic material (SIM) flux) in 8 river catchments in northeast Iceland. Depending on which of their 8 discharge-SIM flux equations is used for calculation, the 350% seasonal increase in river discharge would induce a 350 to 4900% increase in SIM flux over a year. Therefore, high loads of suspended basaltic particles probably flow to the sea with Icelandic rivers as soon as the snow melts, reaching a peak roughly at the same time as the $\text{Li}/\text{Ca}_{\text{shell}}$ annual maximum. These river particles have a high Li content (several ppm [Pogge von Strandmann *et al.*, 2006]), ~ 1 order of magnitude larger than in shells. Although the freshwater inputs likely flow as a thin surface layer ($\sim 10 \text{ m}$ thickness [cf. Astthorsson, 1990; Andrews *et al.*,

2001]), it is likely that suspended material carried by rivers can cross the halocline and settle on the seafloor, thus modifying the chemistry of bottom waters. Consequently, these Li-rich particles may significantly increase $\text{Li}/\text{Ca}_{\text{shell}}$, either directly (if ingested, transferred to the internal fluids, and then incorporated within the shell during biomineralization) or indirectly if they weather after deposition on the seafloor. This hypothesis could be tested in further studies through analyses of the lithium isotope composition of *A. islandica* shells. SIM originating from the weathering of basaltic material has a very low $\delta^7\text{Li}$ value ($\delta^7\text{Li}_{\text{SIM}} = -1.3$ to 7.5‰ in Icelandic rivers [Pogge von Strandmann *et al.*, 2006]) in comparison to seawater ($\delta^7\text{Li}_{\text{seawater}} = 32\text{‰}$ [Huh *et al.*, 1998]). If indeed Li incorporation in shells is linked to Li-rich particle inputs by rivers, then shell aragonite must have a $\delta^7\text{Li}$ several per mil lighter than seawater.

4.3. Conclusions

[37] Lithium is likely incorporated in *A. islandica* aragonitic shells as lithium carbonate Li_2CO_3 ; that is, Li^+ substitutes for Ca^{2+} at the site of calcification in the extrapallial fluid. Several explanations could account for the observed seasonal variations in Li/Ca ratio in shells:

[38] 1. The significant positive relationship found between $\delta^{18}\text{O}_{\text{shell}}$ -derived temperature and $\text{Li}/\text{Ca}_{\text{shell}}$ suggests that seasonal $\text{Li}/\text{Ca}_{\text{shell}}$ variations could be linked to increasing solubility of Li_2CO_3 with decreasing temperature in the extrapallial fluid. However, the strength of this relationship is so weak that temperature-dependent solubility of Li_2CO_3 cannot possibly be the main factor controlling $\text{Li}/\text{Ca}_{\text{shell}}$ variations;

[39] 2. Given the strong and significant positive relationship found between $\text{Li}/\text{Ca}_{\text{shell}}$ and micro-growth increment width, $\text{Li}/\text{Ca}_{\text{shell}}$ may partly be controlled by variations in calcification rate. As this rate is also partly controlled by temperature, it is difficult to make conclusions about the exact importance of Li_2CO_3 solubility in $\text{Li}/\text{Ca}_{\text{shell}}$ variations;

[40] 3. Sandá river discharge and $\text{Li}/\text{Ca}_{\text{shell}}$ presented an intriguing similarity in their seasonal variations. As soon as snow melts in spring, mechanical weathering of basaltic rocks gains intensity due to the increased river discharge, leading to a massive flow of Li-rich silicate particles into the ocean. This phenomenon reaches a peak at the same time as $\text{Li}/\text{Ca}_{\text{shell}}$. We therefore



suggest that this massive input of Li could be trapped in the shell, thus impacting Li/Ca_{shell}.

[41] If indeed Li/Ca_{shell} is mainly controlled by calcification rate, then this ratio may be useful to address seasonal variations in growth rate of bivalve species in which daily growth increments and lines are not easily discernable. In turn, abrupt decreases of Li/Ca_{shell} may be helpful to identify growth retardations, for instance related to the occurrence of toxic phytoplankton blooms in coastal ecosystems. Alternatively, if Li/Ca_{shell} in *A. islandica* is controlled by river inputs of Li-rich silicate particles, it may then be used a proxy for the intensity of mechanical weathering of Icelandic basaltic rocks. This could have exciting perspectives, e.g., to get a better insight about the frequency and intensity of past jökulhlaups (subglacial outburst floods). It may also be interesting to analyze the geochemical composition of recent *A. islandica* shells from the southeast coast of Iceland, where a huge jökulhlaup flowed under the Vatnajökull glacier in 1996 because of the subglacial eruption of the Grímsvötn Volcano. In any event, it is clear from our work that further studies, including $\delta^7\text{Li}_{\text{shell}}$ analyses and experiments under controlled conditions, are needed to better understand Li/Ca_{shell} variations in bivalve shells and to determine if this could be a useful proxy for paleoecological reconstructions.

Acknowledgments

[42] We acknowledge Jens Fiebig (University of Frankfurt, Germany) for isotopic analyses of *Arctica* shells, Chris Romanek (University of Georgia, United States) for $\delta^{18}\text{O}$ analysis of water samples, and Sven Baier for help during dredging in Iceland. Dredging of samples was kindly made possible by Siggeir Stefánsson and Þorgrímur Kjartansson (Hraðfrystistöð Þórshafnar, Iceland). We also express deep appreciation to the Oceanographic Group of the Marine Research Institute of Reykjavik for making their temperature and salinity data freely available on their website (<http://www.hafro.is/Sjora/>) and to the Hydrological Service of the Icelandic National Energy Authority for Sandá River discharge data (data available at <http://www.os.is/>). Thanks are due to the NASA Goddard Institute for Space Studies and especially Gavin Schmidt, Grant Bigg, and Eelco Rohling for their compilation of salinity and $\delta^{18}\text{O}_{\text{water}}$ data (<http://data.giss.nasa.gov/o18data/>) and to the scientists of the VEINS Program who made their salinity and $\delta^{18}\text{O}_{\text{water}}$ data available on the NASA website. This manuscript has greatly benefited from critical reviews and very helpful comments by Katie Matthews and two anonymous reviewers. Financial support for this study was provided by the German Research Foundation (DFG) to Bernd R. Schöne (SCHO 793/4). Julien Thébault gratefully acknowledges the Alexander von Humboldt Foundation (Bonn,

Germany) for the award of a Research Fellowship for Postdoctoral Researchers. This is Geocycles publication 627.

References

- Andrews, J. T., C. Caseldine, N. J. Weiner, and J. Hattón (2001), Late Holocene (ca. 4 ka) marine and terrestrial environmental change in Reykjarfjörður, north Iceland: Climate and/or settlement?, *J. Quat. Sci.*, *16*, 133–143.
- Astthorsson, O. S. (1990), Ecology of the euphausiids *Thysanoessa raschi*, *T. inermis* and *Meganctiphanes norvegica* in Ísafjörð-deep, northwest-Iceland, *Mar. Biol.*, *107*, 147–157, doi:10.1007/BF01313252.
- Broecker, W. S., and T.-H. Peng (Eds.) (1982), *Tracers in the Sea*, 690 pp., Eldigio, Palisades, New York.
- Carré, M., I. Bentaleb, O. Bruguier, E. Ordinoia, N. T. Barrett, and M. Fontugne (2006), Calcification rate influence on trace element concentrations in aragonitic bivalve shells: Evidences and mechanisms, *Geochim. Cosmochim. Acta*, *70*, 4906–4920, doi:10.1016/j.gca.2006.07.019.
- Carriker, M. R., C. P. Swann, J. Ewart, and C. L. Counts III (1996), Ontogenetic trends of elements (Na to Sr) in prismatic shell of living *Crassostrea virginica* (Gmelin) grown in three ecologically dissimilar habitats for 28 weeks: A proton probe study, *J. Exp. Mar. Biol. Ecol.*, *201*, 87–135, doi:10.1016/0022-0981(96)00013-5.
- Chauvaud, L., A. Lorrain, R. B. Dunbar, Y.-M. Paulet, G. Thouzeau, F. Jean, J.-M. Guarini, and D. Mucciarone (2005), Shell of the Great Scallop *Pecten maximus* as a high-frequency archive of paleoenvironmental changes, *Geochem. Geophys. Geosyst.*, *6*, Q08001, doi:10.1029/2004GC000890.
- Craig, C.-A., K. E. Jarvis, and L. J. Clarke (2000), An assessment of calibration strategies for the quantitative and semi-quantitative analysis of calcium carbonate matrices by laser ablation-inductively coupled plasma-mass spectrometry (LA-ICP-MS), *J. Anal. At. Spectrom.*, *15*, 1001–1008, doi:10.1039/b002097o.
- Delaney, M. L., A. W. H. Bé, and E. A. Boyle (1985), Li, Sr, Mg, and Na in foraminiferal calcite shells from laboratory culture, sediment traps, and sediment cores, *Geochim. Cosmochim. Acta*, *49*, 1327–1341, doi:10.1016/0016-7037(85)90284-4.
- Delaney, M. L., B. N. Popp, C. G. Lepzelter, and T. F. Anderson (1989), Lithium-to-calcium ratios in modern, Cenozoic, and Paleozoic articulate brachiopod shells, *Paleoceanography*, *4*, 681–691, doi:10.1029/PA004i006p00681.
- Dick, D., E. Philipp, M. Kriewis, and D. Abele (2007), Is the umbo matrix of bivalve shells (*Laternula elliptica*) a climate archive?, *Aquat. Toxicol.*, *84*, 450–456, doi:10.1016/j.aquatox.2007.07.005.
- Éplé, V. M. (2004), High-resolution climate reconstruction for the Holocene based on growth chronologies of the bivalve *Arctica islandica* from the North Sea, Ph.D. thesis, 101 pp., Univ. of Bremen, Bremen, Germany, 17 Dec.
- Epstein, S., R. Buchsbaum, H. A. Lowenstam, and H. C. Urey (1953), Revised carbonate-water isotopic temperature scale, *Geol. Soc. Am. Bull.*, *64*, 1315–1326, doi:10.1130/0016-7606(1953)64[1315:RCITS]2.0.CO;2.
- Fiebig, J., B. R. Schöne, and W. Oschmann (2005), High-precision oxygen and carbon isotope analysis of very small (10–30 μg) amounts of carbonates using continuous flow isotope ratio mass spectrometry, *Rapid Commun. Mass Spectrom.*, *19*, 2355–2358, doi:10.1002/rcm.2060.



- Gillikin, D. P., A. Lorrain, J. Navez, J. W. Taylor, L. André, E. Keppens, W. Baeyens, and F. Dehairs (2005), Strong biological controls on Sr/Ca ratios in aragonitic marine bivalve shells, *Geochem. Geophys. Geosyst.*, *6*, Q05009, doi:10.1029/2004GC000874.
- Gislason, S. R., et al. (2009), Direct evidence of the feedback between climate and weathering, *Earth Planet. Sci. Lett.*, *277*, 213–222, doi:10.1016/j.epsl.2008.10.018.
- Grossman, E. L., and T.-L. Ku (1986), Oxygen and carbon isotope fractionation in biogenic aragonite: Temperature effects, *Chem. Geol.*, *59*, 59–74, doi:10.1016/0009-2541(86)90044-6.
- Hall, J. M., and L.-H. Chan (2004), Li/Ca in multiple species of benthic and planktonic foraminifera: Thermocline, latitudinal, and glacial-interglacial variation, *Geochim. Cosmochim. Acta*, *68*, 529–545, doi:10.1016/S0016-7037(03)00451-4.
- Hathorne, E. C., and R. H. James (2006), Temporal record of lithium in seawater: A tracer for silicate weathering?, *Earth Planet. Sci. Lett.*, *246*, 393–406, doi:10.1016/j.epsl.2006.04.020.
- Henderson, G. M. (2002), New oceanic proxies for paleoclimate, *Earth Planet. Sci. Lett.*, *203*, 1–13, doi:10.1016/S0012-821X(02)00809-9.
- Hoefs, J., and M. Sywall (1997), Lithium isotope composition of quaternary and tertiary biogenic carbonates and a global lithium isotope balance, *Geochim. Cosmochim. Acta*, *61*, 2679–2690, doi:10.1016/S0016-7037(97)00101-4.
- Hopkins, T. S. (1991), The GIN Sea—A synthesis of its physical oceanography and literature review 1972–1985, *Earth Sci. Rev.*, *30*, 175–318, doi:10.1016/0012-8252(91)90001-V.
- Huh, Y., L.-H. Chan, L. Zhang, and J. M. Edmond (1998), Lithium and its isotopes in major world rivers: Implications for weathering and the oceanic budget, *Geochim. Cosmochim. Acta*, *62*, 2039–2051, doi:10.1016/S0016-7037(98)00126-4.
- Hut, G. (1987), Consultants' group meeting on stable isotope reference samples for geochemical and hydrological investigations, report to the Director General, 44 pp., Int. At. Energy Agency, Vienna.
- Jones, D. S. (1983), Sclerochronology: Reading the record of the mollusk shell, *Am. Sci.*, *71*, 384–391.
- Jones, D. S. (1998), Isotopic determination of growth and longevity on fossil and modern invertebrates, *Palaeontol. Soc. Pap.*, *4*, 37–67.
- Kilada, R. W., S. E. Campana, and D. Roddick (2007), Validated age, growth, and mortality estimates of the ocean quahog (*Arctica islandica*) in the western Atlantic, *ICES J. Mar. Sci.*, *64*, 31–38.
- Kurosawa, M., S. E. Jackson, and S. Sueno (2002), Trace element analysis of NIST SRM 614 and 616 glass reference materials by laser ablation microprobe-inductively coupled plasma-mass spectrometry, *Geostand. Geoanal. Res.*, *26*, 75–84, doi:10.1111/j.1751-908X.2002.tb00625.x.
- Li, Y.-H. (Ed) (2000), *A Compendium of Geochemistry: From Solar Nebula to the Human Brain*, 440 pp., Princeton Univ. Press, Princeton, N. J.
- Liehr, G. A., M. L. Zettler, T. Leipe, and G. Witt (2005), The ocean quahog *Arctica islandica* L.: A bioindicator for contaminated sediments, *Mar. Biol.*, *147*, 671–679, doi:10.1007/s00227-005-1612-y.
- Lindh, U., H. Mutvei, T. Sunde, and T. Westermark (1988), Environmental history told by mussel shells, *Nucl. Instrum. Methods Phys. Res., Sect. B*, *30*, 388–392, doi:10.1016/0168-583X(88)90030-4.
- Lingard, S. M., R. D. Evans, and B. P. Bourgoin (1992), Method for the estimation of organic-bound and crystal-bound metal concentrations in bivalve shells, *Bull. Environ. Contam. Toxicol.*, *48*, 179–184, doi:10.1007/BF00194369.
- Longerich, H. P., S. E. Jackson, and D. Günther (1996), Laser ablation inductively coupled plasma mass spectrometric transient signal data acquisition and analyte concentration calculation, *J. Anal. At. Spectrom.*, *11*, 899–904, doi:10.1039/ja9961100899.
- Marchitto, T. M., G. A. Jones, G. A. Goodfriend, and C. R. Weidman (2000), Precise temporal correlation of Holocene mollusk shells using sclerochronologie, *Quat. Res.*, *53*, 236–246, doi:10.1006/qres.1999.2107.
- Marin, F., and G. Luquet (2004), Molluscan shell proteins, *C. R. Palevol*, *3*, 469–492, doi:10.1016/j.crpv.2004.07.009.
- Marriott, C. S., G. M. Henderson, R. Crompton, M. Staubwasser, and S. Shaw (2004a), Effect of mineralogy, salinity, and temperature on Li/Ca and Li isotope composition of calcium carbonate, *Chem. Geol.*, *212*, 5–15, doi:10.1016/j.chemgeo.2004.08.002.
- Marriott, C. S., G. M. Henderson, N. S. Belshaw, and A. W. Tudhope (2004b), Temperature dependence of $\delta^7\text{Li}$, $\delta^{44}\text{Ca}$ and Li/Ca during growth of calcium carbonate, *Earth Planet. Sci. Lett.*, *222*, 615–624, doi:10.1016/j.epsl.2004.02.031.
- McCrea, J. M. (1950), On the isotopic chemistry of carbonates and a paleotemperature scale, *J. Chem. Phys.*, *18*, 849–857, doi:10.1063/1.1747785.
- Montagna, P., M. McCulloch, C. Mazzoli, S. Silenzi, and S. Schiaparelli (2006), Li/Ca ratios in the Mediterranean non-tropical coral *Cladocora caespitosa* as a potential paleothermometer, *Geophys. Res. Abstr.*, *8*, abstract 03695.
- Okumura, M., and Y. Kitano (1986), Coprecipitation of alkali metal ions with calcium carbonate, *Geochim. Cosmochim. Acta*, *50*, 49–58, doi:10.1016/0016-7037(86)90047-5.
- Pannella, G., and C. McClintock (1968), Biological and environmental rhythms reflected in molluscan shell growth, *J. Paleontol.*, *42*, 64–80.
- Pearce, N. J. G., W. T. Perkins, J. A. Westgate, M. P. Gorton, S. E. Jackson, C. R. Neal, and S. P. Chenery (1997), A compilation of new and published major and trace element data for NIST SRM 610 and NIST SRM 612 glass reference materials, *Geostand. Geoanal. Res.*, *21*, 115–144, doi:10.1111/j.1751-908X.1997.tb00538.x.
- Pogge von Strandmann, P. A. E., K. W. Burton, R. H. James, P. van Calsteren, S. R. Gislason, and F. Mokadem (2006), Riverine behaviour of uranium and lithium isotopes in an actively glaciated basaltic terrain, *Earth Planet. Sci. Lett.*, *251*, 134–147, doi:10.1016/j.epsl.2006.09.001.
- Scherrer, B. (1984), *Biostatistiques*, 850 pp., G. Morin Ed., Montreal, Que., Canada.
- Schmidt, G. A., G. R. Bigg, and E. J. Rohling (1999), Global seawater oxygen-18 database, <http://data.giss.nasa.gov/o18data/>, Goddard Inst. for Space Stud., New York.
- Schöne, B. R. (2008), The curse of physiology—Challenges and opportunities in the interpretation of geochemical data from mollusk shells, *Geo Mar. Lett.*, *28*, 269–285, doi:10.1007/s00367-008-0114-6.
- Schöne, B. R., W. Oschmann, J. Rössler, A. D. Freyre Castro, S. D. Houk, I. Kröncke, W. Dreyer, R. Janssen, H. Rumohr, and E. Dunca (2003), North Atlantic Oscillation dynamics recorded in shells of a long-lived bivalve mollusk, *Geology*, *31*, 1037–1040, doi:10.1130/G20013.1.
- Schöne, B. R., A. D. Freyre Castro, J. Fiebig, S. D. Houk, W. Oschmann, and I. Kröncke (2004), Sea surface water temperatures over the period 1884–1983 reconstructed from oxygen isotope ratios of a bivalve mollusk shell (*Arctica islandica*, southern North Sea), *Palaeogeogr. Palaeoclimatol. Palaeoecol.*, *212*, 215–232.



- Schöne, B. R., S. D. Houk, A. D. Freyre Castro, J. Fiebig, W. Oschmann, I. Kröncke, W. Dreyer, and F. Gosselck (2005a), Daily growth rates in shells of *Arctica islandica*: Assessing sub-seasonal environmental controls on a long-lived bivalve mollusk, *Palaios*, *20*, 78–92, doi:10.2110/palo.2003.p03-101.
- Schöne, B. R., J. Fiebig, M. Pfeiffer, R. Gleß, J. Hickson, A. L. A. Johnson, W. Dreyer, and W. Oschmann (2005b), Climate records from a bivalved Methuselah (*Arctica islandica*, Mollusca; Iceland), *Palaeogeogr. Palaeoclimatol. Palaeoecol.*, *228*, 130–148, doi:10.1016/j.palaeo.2005.03.049.
- Schöne, B. R., M. Pfeiffer, T. Pohlmann, and F. Siegmund (2005c), A seasonally resolved bottom-water temperature record for the period AD 1866–2002 based on shells of *Arctica islandica* (Mollusca, North Sea), *Int. J. Climatol.*, *25*, 947–962, doi:10.1002/joc.1174.
- Schöne, B. R., E. Dunca, J. Fiebig, and M. Pfeiffer (2005d), Mutvei's solution: An ideal agent for resolving microgrowth structures of biogenic carbonates, *Palaeogeogr. Palaeoclimatol. Palaeoecol.*, *228*, 149–166, doi:10.1016/j.palaeo.2005.03.054.
- Smith, S. H., D. D. Williams, and R. R. Miller (1971), Solubility of lithium carbonate at elevated temperatures, *J. Chem. Eng. Data*, *16*, 74–75, doi:10.1021/je60048a022.
- Stecher, H. A., III, D. E. Krantz, C. J. Lord III, G. W. Luther III, and K. W. Bock (1996), Profiles of strontium and barium in *Mercenaria mercenaria* and *Spisula solidissima* shells, *Geochim. Cosmochim. Acta*, *60*, 3445–3456, doi:10.1016/0016-7037(96)00179-2.
- Stoffyn-Egli, P., and F. T. Mackenzie (1984), Mass balance of dissolved lithium in the oceans, *Geochim. Cosmochim. Acta*, *48*, 859–872, doi:10.1016/0016-7037(84)90107-8.
- Thébault, J., L. Chauvaud, J. Clavier, J. Guarini, R. B. Dunbar, R. Fichez, D. A. Mucciarone, and E. Morize (2007), Reconstruction of seasonal temperature variability in the tropical Pacific Ocean from the shell of the scallop, *Comptopallium radula*, *Geochim. Cosmochim. Acta*, *71*, 918–928, doi:10.1016/j.gca.2006.10.017.
- Thébault, J., L. Chauvaud, S. L'Helguen, J. Clavier, A. Barats, S. Jacquet, C. Pécheyran, and D. Amouroux (2009), Barium and molybdenum records in bivalve shells: Geochemical proxies for phytoplankton dynamics in coastal environments?, *Limnol. Oceanogr.*, *54*, 1002–1014.
- Thorarinsdóttir, G. G. (2000), Annual gametogenic cycle in ocean quahog, *Arctica islandica* from north-western Iceland, *J. Mar. Biol. Assoc. U. K.*, *80*, 661–666, doi:10.1017/S0025315400002484.
- Thorarinsdóttir, G. G., and L. D. Jacobson (2005), Fishery biology and biological reference points for management of ocean quahogs (*Arctica islandica*) off Iceland, *Fish. Res.*, *75*, 97–106, doi:10.1016/j.fishres.2005.04.010.
- Toland, H., B. Perkins, N. Pearce, F. Keenan, and M. J. Leng (2000), A study of sclerochronology by laser ablation ICP-MS, *J. Anal. At. Spectrom.*, *15*, 1143–1148, doi:10.1039/b002014l.
- Van Achterbergh, E., C. G. Ryan, S. E. Jackson, and W. L. Griffin (2001), Data reduction software for LA-ICP-MS, in *Laser Ablation-ICPMS in the Earth Sciences: Principles and Applications*, edited by P. J. Sylvester, pp. 239–243, *Short Course Ser.*, vol. 29, Mineral. Assoc. of Can., Ottawa, Ont., Canada.
- Vander Putten, E., F. Dehairs, E. Keppens, and W. Baeyens (2000), High resolution distribution of trace elements in the calcite shell layer of modern *Mytilus edulis*: Environmental and biological controls, *Geochim. Cosmochim. Acta*, *64*, 997–1011, doi:10.1016/S0016-7037(99)00380-4.
- Vigier, N., S. R. Gislason, K. W. Burton, R. Millot, and F. Mokadem (2009), The relationship between riverine lithium isotope composition and silicate weathering rates in Iceland, *Earth Planet. Sci. Lett.*, *287*, 434–441, doi:10.1016/j.epsl.2009.08.026.
- Wanamaker, A. D., J. Heinemeier, J. D. Scourse, C. A. Richardson, P. G. Butler, J. Eiriksson, and K. L. Knudsen (2008a), Very-long lived molluscs confirm 17th century AD tephra-based radiocarbon reservoir ages for north Icelandic shelf waters, *Radiocarbon*, *50*, 399–412.
- Wanamaker, A. D., K. J. Kreutz, B. R. Schöne, N. Pettigrew, H. W. Borns, D. S. Introne, D. Belknap, K. A. Maasch, and S. Feindel (2008b), Coupled North Atlantic slope water forcing on Gulf of Maine temperatures over the past millennium, *Clim. Dyn.*, *31*, 183–194, doi:10.1007/s00382-007-0344-8.
- Wefer, G., W. H. Berger, J. Bijma, and G. Fischer (1999), Clues to ocean history: A brief overview of proxies, in *Use of Proxies in Paleooceanography: Examples From the South Atlantic*, edited by G. Fischer and G. Wefer, pp. 1–68, Springer, Berlin.
- Weidman, C. R., G. A. Jones, and K. C. Lohmann (1994), The long-lived mollusc *Arctica islandica*: A new paleoceanographic tool for the reconstruction of bottom temperatures for the continental shelves of the northern North Atlantic Ocean, *J. Geophys. Res.*, *99*, 18,305–18,314, doi:10.1029/94JC01882.
- Witbaard, R. (1997), Tree of the sea: The use of the internal growth lines in the shell of *Arctica islandica* (Bivalvia, Mollusca) for the retrospective assessment of marine environmental change, Ph.D. thesis, 157 pp., Rijksuniv. Groningen, Groningen, Netherlands, 30 May.